Induced Quantum Dots and Wires: Electron Storage and Delivery

S. Bednarek, B. Szafran, R. J. Dudek, and K. Lis

Faculty of Physics and Applied Computer Science, AGH University of Science and Technology, al. Mickiewicza 30, 30-059 Kraków, Poland

(Received 24 July 2007; published 28 March 2008)

We show that quantum dots and quantum wires are formed underneath metal electrodes deposited on a planar semiconductor heterostructure containing a quantum well. The confinement is due to the self-focusing mechanism of an electron wave packet interacting with the charge induced on the metal surface. Induced quantum wires guide the transfer of electrons along metal paths and induced quantum dots store the electrons in specific locations of the nanostructure. Induced dots and wires can be useful for devices operating on the electron spin. An application for a spin readout device is proposed.

DOI: 10.1103/PhysRevLett.100.126805 PACS numbers: 73.21.La, 73.40.Gk, 73.63.Nm

Planar nanodevices containing single [1–6], double [7–10], and multiple [11,12] laterally coupled quantum dots with the confinement potential tuned by electrodes deposited on top of the semiconductor heterostructure are at present extensively studied in both theory and experiment in the context of their application to quantum gates using electron spins as quantum bits. Recent advances include the demonstration that the electron spin can be set and read out [2,4–9,13] as well as rotated [6,13]. In a quantum gate working on the electron spins [14] the single qubit operations are to be performed with an electron transfer to a high g factor region or to a ferromagnetic quantum dot where the electron spin is rotated by microwave radiation. In this Letter we present an idea for the control of the electron localization and its transfer between specific locations within the nanodevice. The idea is based on the self-focusing mechanism of an electron wave packet near a conductor surface [15–17] which as we show below allows us to exclude scattering during the electron transfer and warrants the electron delivery to a specific location in the device with a 100% probability. An application of the present idea for a spin-charge converter is demonstrated.

In conventional planar nanodevices [1,2] a negative potential is applied to the gate electrodes to deplete the two-dimensional electron gas underneath. In the variant of the structure proposed below the role of the electrodes is different: a single quantum-well-confined electron becomes self-trapped below the conductor by the potential of the charge that it induces on the metal surface. The response potential of the electron gas of the conductor contains a component of lateral confinement which localizes the quantum-well-confined electron in the form of a wave packet that moves parallel to the metal preserving its shape as an electron soliton [15,16]. The packet was called [17] an *inducton* since the focusing potential stems from the charge induced in the electron gas. The inducton possesses mixed quantum and classical properties. It is described by a wave function of both spatial and spin coordinates whose time evolution is described by the Schrödinger equation. On the other hand, the inducton moves as a stable wave packet of a finite size and its transition probability in transport through potential barriers is binary (0 or 1) [16], like for a classical particle.

In Ref. [16] we discussed a structure of planar infinite layers of metal, insulator (or semiconducting blocking barrier), and a quantum well in which the inducton was formed. Because of the translational symmetry the inducton can be formed at any place under an infinite metal plate and travel in any direction within the quantum well. In this Letter we show that a metal electrode of a finite size is also able to trap an electron underneath it. For the size of the electrode comparable to the inducton radius the transverse motion of the packet is frozen and the induced charge creates a confinement potential similar to the quantum dot potential. A rectangular metal electrode of length larger than the size of the self-focused wave packet leaves the inducton a single degree of freedom for motion along the metal path which therefore forms an induced quantum wire within the quantum well.

The induced potential calculated within the quantum linear response theory is well approximated by the response of an ideal (classical) conductor [16,17]. Therefore, the induced potential can be quite accurately evaluated by the classical electrodynamics. Let us consider a nanodevice presented in Fig. 1. For an infinite metal plate the induced potential can be evaluated with the image

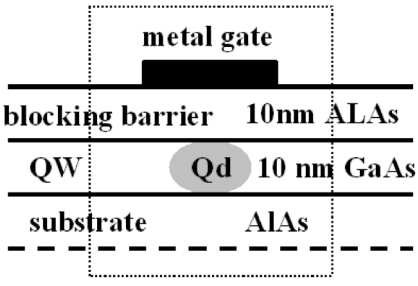

FIG. 1. Cross section of a nanodevice generating an induced quantum dot or wire. Dotted line shows the boundaries of the computational box.

charge method [16], which greatly simplifies the calculations but is no longer applicable for metal plates of finite size, for which the induced potential has to be calculated from the Poisson equation. For that reason we apply the theory used previously in modeling of electrostatic quantum dots [18] which describes experiments with a remarkable accuracy. The presence of the metal (see Fig. 1) introduces fixed potential value in the boundary conditions at the conducting surface. All the nanodevice is contained in a rectangular computational box (see the dotted line in Fig. 1). At the surface of the box we require the normal component of the electric field to vanish. The size of the box is taken large enough that for an infinite metal plate we reproduce the image charge potential. We solve the Poisson equation

$$\nabla^2\Phi(\mathbf{r}) = -\frac{1}{\epsilon\epsilon_0}\rho(\mathbf{r}), \tag{1}$$

where the charge density is expressed by the electron wave function $\psi(\mathbf{r})$ and the electron charge $-e$: $\rho(\mathbf{r}) = -e|\psi(\mathbf{r})|^2$. According to the superposition principle the calculated total potential Φ is a sum of contributions stemming from two sources $\Phi(\mathbf{r}) = \phi_1(\mathbf{r}) + \phi_2(\mathbf{r})$, where ϕ_1 is directly due to the wave packet charge density distribution

$$\phi_1(\mathbf{r}) = \frac{-e}{4\pi\epsilon\epsilon_0}\int d\mathbf{r}'\frac{\rho(\mathbf{r}')}{|\mathbf{r}-\mathbf{r}'|}, \tag{2}$$

and the second component is due to the charge induced on the electrode which creates the lateral confinement for the electron localized in the quantum well. Given the total potential Φ and the potential of the electron packet ϕ_1 the induced potential ϕ_2 is calculated according to

$$\phi_2(\mathbf{r}) = \Phi(\mathbf{r}) - \phi_1(\mathbf{r}). \tag{3}$$

For the nanostructure of Fig. 1 the motion of the electron in the growth direction is frozen by the strong vertical confinement which can be eliminated from the Schrödinger equation thus taking a two dimensional form

$$H = -\frac{\hbar^2}{2m}\left(\frac{\partial^2}{\partial x^2} + \frac{\partial^2}{\partial y^2}\right) - e\phi_2(x, y, z_0), \tag{4}$$

where z_0 is the center of the quantum well. In the eigenequation $H\psi = E\psi$, E is the single-electron energy [16]. The total energy is obtained [16] by subtracting half of the interaction energy of the inducton with the induced potential:

$$E^{\text{tot}} = E + \frac{e}{2}\int dxdy|\psi(x, y)|^2\phi_2(x, y, z_0). \tag{5}$$

The ϕ_2 potential and the wave function ψ are mutually dependent so the problem is solved in a self-consistent iteration.

Let us assume that the metal electrode deposited on top of the semiconductor (see Fig. 1) is of a square shape with side length b. We solve Eqs. (1)–(5) and evaluate the average diameter of the electron wave packet

$$D = 2\int dxdy\sqrt{(x-x_0)^2 + (y-y_0)^2}|\psi(x, y)|^2, \tag{6}$$

where (x_0, y_0) are the coordinates of the center of the metal square. GaAs electron effective mass $m = 0.067m_0$ and dielectric constant $\epsilon = 12.5$ are adopted.

The single-electron energy, the total energy and the packet diameter are plotted as function of b in Fig. 2(a). Both the energies are negative (for any b) and decrease with growing b reaching the free inducton (electron wave packet under an infinite metal plate) limit [16]. The limit is obtained for b larger than the free inducton radius. The packet diameter is a non monotonic function of b. For small plate the packet is large. The packet localization is the strongest for $b^{\text{dot}}_{\text{min}} = 70$ nm and for $b > b^{\text{dot}}_{\text{min}}$ the diameter grows to the free inducton limit. Soon after the minimal diameter is reached the energies saturate as function of b. Note that the minimal diameter is nearly equal to $b^{\text{dot}}_{\text{min}}$ (for the charge density and the size of the plate see Fig. 2(b)]. The $b^{\text{dot}}_{\text{min}}$ value is optimal for the proposed applications of electron storage and transfer.

Similar calculation was performed for the electrode in form of a metal bar that is infinite in the x direction and of width b in the y direction (it will be referred to as a current path). Figure 2(c) shows both the energies and the size of

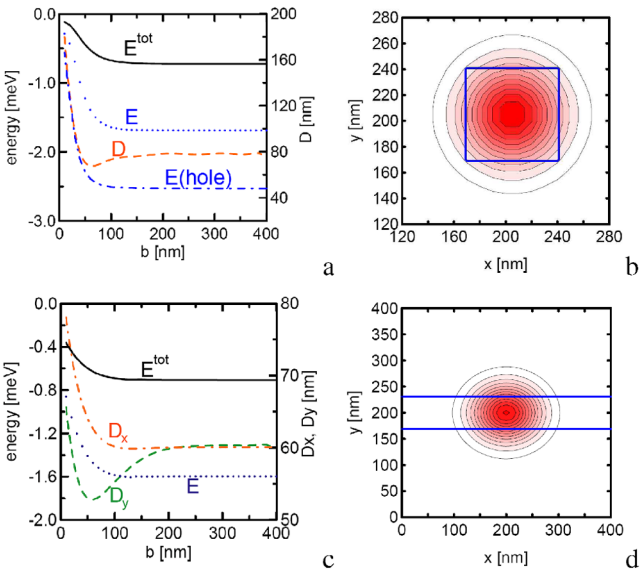

FIG. 2 (color online). (a) Total energy E^{tot}, single-electron energy E, and diameter of the wave packet D for a quantum dot induced by square metal plate of side length b. Dash-dotted curve shows the eigenvalue E for a heavy hole inducton ($m = 0.45m_0$). (b) Electron density in the quantum dot induced by square metal plate with $b = 70$ nm. (c) E^{tot}, E and packet length along x and y direction (D_x, D_y) for a quantum wire induced by an infinite metal bar of width b. (d) Charge density of the wave packet confined under the metal bar of width $b = 50$ nm.

the packet in both directions of the quantum wire

$$D_x = 2\int dxdy|x - x_0||\psi(x, y)|^2, \quad (7)$$

$$D_y = 2\int dxdy|y - y_0||\psi(x, y)|^2. \quad (8)$$

Quite remarkably, values of D_x and D_y are close, although only D_y has a minimum as a function of b. The strongest focusing appears for the current path of width $b_{\min}^{\text{wire}} =$ 50 nm, adopted as optimal in the following. The charge distribution for $b = b_{\min}^{\text{wire}}$ plotted in Fig. 2(d) shows that the packet is more strongly localized in the direction perpendicular to the path.

In the calculations discussed above the stationary eigenproblem of Hamiltonian (4) was solved by the evolution in the imaginary time [19] which leads to formation of the ground state wave function. A slight modification of the approach allows the investigation of the evolution in the real time. For that purpose the time dependent Schrödinger equation is solved:

$$d\psi(\mathbf{r}, t) = \frac{i}{\hbar}H(\mathbf{r}, t)\psi(\mathbf{r}, t)dt. \quad (9)$$

The dependence of the Hamiltonian on time appears for a moving inducton due to the time dependence of the electron density which enters Eqs. (1) and (2) $\rho(\mathbf{r}, t) = -e|\psi(\mathbf{r}, t)|^2$. The time dependence of the potential is determined by Eqs. (1)–(3) solved for each time step (9).

Let us consider a nanodevice whose cross section agrees with the schematic of Fig. 1 and the top view is displayed in Fig. 3(b). On the surface of the structure we have three electrodes separated by gaps of 20 nm. Quantum dots are formed below square electrodes e_1 and e_3 both of size 70 nm × 70 nm. The middle electrode e_2 (50 nm × 500 nm) is supposed to induce a quantum wire which should guide an electron from under e_1 to e_3.

We assume that the electron is confined below e_1 for a time long enough to relax to the ground state. In the simulation it is achieved by the imaginary time evolution for potentials of the electrodes (the Schottky barrier neglected): $V_1 = 0.0$ mV, $V_2 = V_3 = -0.1$ mV (V_1, V_2, V_3 are the potentials applied to e_1, e_2, e_3 electrodes, respectively). After the inducton relaxes to the ground state we change the applied voltages putting $V_1 = -0.1$ mV, $V_2 =$ 0.0 mV, $V_3 = -0.1$ mV and we start the evolution in the real time. The inversed $V_1 - V_2$ potential difference gently sets the electron in motion. The electron gains the kinetic energy passing from below e_1 to e_2. Next it goes along e_2 with a constant kinetic energy eventually reaching the quantum dot induced under e_3. At that moment V_2 voltage is switched to $V_2 = -0.15$ mV to confine the electron permanently under e_3. The traveling electron density is presented in Fig. 3(b) for several moments in time. In Fig. 3(a) $|\psi(x, y_0, t)|^2$ is plotted for $y_0 = 100$ nm set at the symmetry axis of the proposed setup. We can see that the inducton is accelerated between e_1 and e_2 (see the curved shape of the density plot in Fig. 3(a) between $x =$ 100 and 200 nm). Then it moves with a constant velocity under e_2 [note increased localization of the packet when under e_2]. Finally, the packet gets under e_3 and is trapped there when V_2 is switched to negative. The oscillations observed in Fig. 3(a) for $t > 50$ ps are due to the residual kinetic energy which is not lost when the inducton is trapped under e_3. The crucial point of the presented results is that the electron was transferred from one dot to the other with a 100% probability which is due to the self-focusing mechanism.

Let us consider a similar structures but with varied shape of the electrodes (blue lines in Fig. 4). The middle elec-

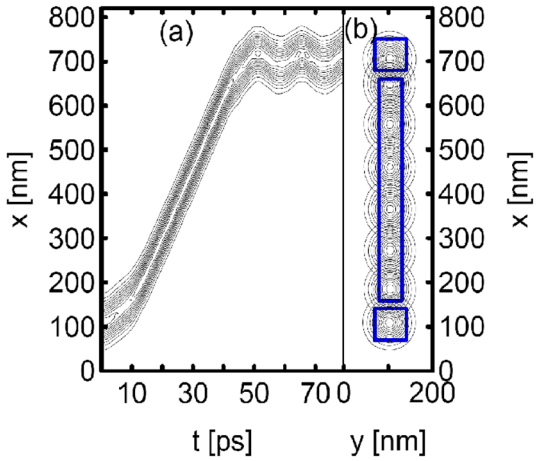

FIG. 3 (color online). (a) Electron charge density as function of the x-variable and time calculated at the symmetry axis ($y = y_0 = 100$ nm) of the electrode configuration presented with blue lines in (b). The contour plots in (b) display the charge density at subsequent moments in time.

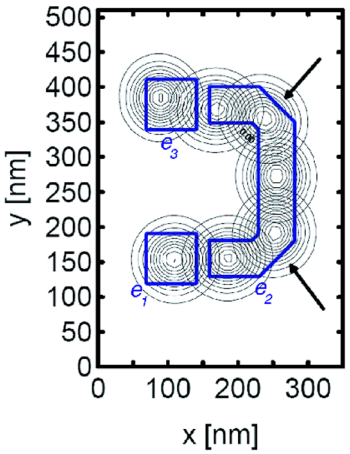

FIG. 4 (color online). Snapshots of the time evolution of the electron density following the path which is not straight like in Fig. 3(b) but broken twice. The arrows indicate the cut corners of the metal path. The electron leaves the quantum dot induced under the e_1 electrode and goes to the quantum dot under e_3.

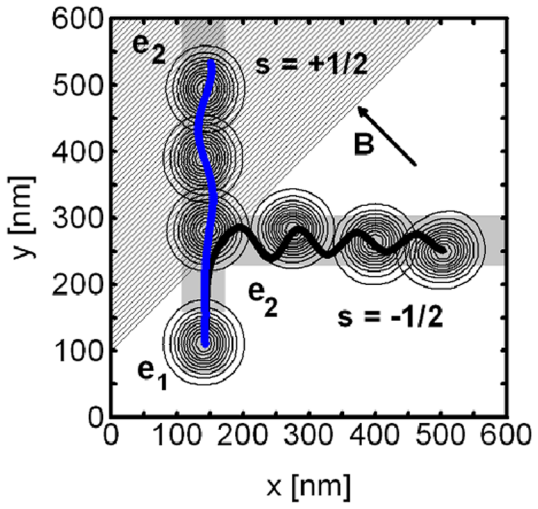

FIG. 5 (color online). Snapshots of the time simulations for the $Mn_xGa_{1-x}As$ quantum well with position dependent Mn concentration. In the shaded region (left upper corner) $x = 0.0013$ and outside of it $x = 0$. The magnetic field polarizing the Mn spins is perpendicular to the interface of pure GaAs. The gray region denoted by e_1 is a square electrode forming an induced quantum dot. Induced wires are formed below e_2 electrode (the other gray region). Thick black and blue lines show the trajectory of the wave packet of spin down ($s = -\frac{1}{2}$) and up ($s = +\frac{1}{2}$), respectively, (s is the spin component parallel to the magnetic field).

trode turns under right angles to force the inducton to change direction of its velocity vector. Several snapshots of the electron density evolution are shown in Fig. 4 with contours. It turns out that the electron can be guided under any place in the structure also along curved paths. Note the cut corner edges of the current path marked in Fig. 4 with arrows which allows the electron to change the motion direction with equal incident and reflection angles. For an uncut edge (turning at a 90° angle) the electron is reflected back to e_1.

The presented effect of the guided electron-transfer can be used in systems operating on the spins of electrons. Figure 5 presents result of simulation in which the composition of the quantum well is modified. Namely, the induced quantum wire enters under a 45° angle a paramagnetic semiconductor region formed by $Mn_xGa_{1-x}As$ ($x = 0.0013$). The Mn spins are ordered by the magnetic field of 2 T which is applied within the quantum well plane (see Fig. 1) perpendicular to the interface of pure GaAs and MnGaAs. The electron of a spin parallel (antiparallel) to the field perceives the MnGaAs region as a quantum well (barrier) 0.058 meV deep (high) [20]. The gray regions in Fig. 5 show the electrodes. Under a small electrode e_1 a quantum dot is formed in which an electron is initially trapped. Next a potential of $V = -0.05$ mV is applied to e_1 with respect to the electrode e_2. An inducton with spin down is totally reflected from the MnGaAs/GaAs interface and goes to the right, while the electron with spin up is only slightly accelerated at the interface and continues going nearly parallel to the y axis.

The system presented in Fig. 5 can be used as a spin-charge converter for the spin-readout-devices. It can also be used for spin accumulation [21].

To conclude, we presented a design for a planar semiconductor structure with a quantum well and electrodes separated by a tunnel barrier in which induced quantum dots and quantum wires are formed. The dots store the electrons in specific points of the nanostructure and the paths assist in the transport of the electrons between chosen locations in the device. The electron is kept in the stable wave packet (inducton state) by the self-focusing mechanism, which also assists in the transport leading to a 100% probability of passing through potential cavities or barriers. The combination of semiclassical transport properties of the inducton with its spin degree of freedom is likely to become useful for the spin operating devices.

This work was supported by the State Committee for Scientific Research (KBN) under Grant No. 1P03B 002 27.

[1] R. C. Ashoori *et al.*, Phys. Rev. Lett. **68**, 3088 (1992); N. B. Zhitenev *et al.*, Phys. Rev. Lett. **79**, 2308 (1997).
[2] J. M. Elzermann *et al.*, Nature (London) **430**, 431 (2004).
[3] D. K. Ferry, R. Atkins, and J. P. Bird, Phys. Rev. Lett. **93**, 026803 (2004).
[4] R. Hanson *et al.*, Phys. Rev. Lett. **94**, 196802 (2005).
[5] T. Meunier *et al.*, Phys. Rev. B **74**, 195303 (2006).
[6] F. H. L. Koppens *et al.*, Nature (London) **442**, 766 (2006).
[7] T. Hatano *et al.*, Phys. Rev. Lett. **93**, 066806 (2004).
[8] H. A. Engel *et al.*, Phys. Rev. Lett. **93**, 106804 (2004).
[9] J. R. Petta *et al.*, Science **309**, 2180 (2005).
[10] L. P. Kouwenhouven *et al.*, Phys. Status Solidi B **243**, 3682 (2006).
[11] T. Ihn *et al.*, New J. Phys. **9**, 111 (2007).
[12] A. Vidan *et al.*, Appl. Phys. Lett. **85**, 3602 (2004); J. Supercond. **18**, 223 (2005).
[13] W. A. Coish and D. Loss, Phys. Rev. B **75**, 161302 (2007).
[14] D. Loss and D. P. Divincenzo, Phys. Rev. A **57**, 120 (1998).
[15] K. Yano and D. K. Ferry, Superlattices Microstruct. **11**, 61 (1992).
[16] S. Bednarek, B. Szafran, and K. Lis, Phys. Rev. B **72**, 075319 (2005).
[17] S. Bednarek and B. Szafran, Phys. Rev. B **73**, 155318 (2006).
[18] S. Bednarek *et al.*, Phys. Rev. B **61**, 4461 (2000); **64**, 195303 (2001); **68**, 155333 (2003).
[19] K. T. Davies *et al.*, Nucl. Phys. **A342**, 111 (1980).
[20] M. Poggio *et al.*, Phys. Rev. B **72**, 235313 (2005).
[21] B. K. Nikolić *et al.*, Phys. Rev. Lett. **95**, 046601 (2005); M. Governale and U. Zülicke, Phys. Rev. B **66**, 073311 (2002).